Research Square

Preprints are preliminary reports that have not undergone peer review.
They should not be considered conclusive, used to inform clinical practice,
or referenced by the media as validated information.

Mechanical, Water Absorption and Morphological Properties of Nitric Acid-modified Short Carbon Fiber Reinforced Acrylonitrile Butadiene Styrene Composites

Lixiang He
Tianjin University of Technology and Education
Quan Wang
wangquan@tute.edu.cn
Tianjin University of Technology and Education
Tuo Cheng
Tianjin University of Technology and Education
Qun Zhang
Tianjin University of Technology and Education

Research Article

Keywords: short carbon fiber, nitric acid modification, ABS composites, mechanical properties, water absorption, microstructure

Posted Date: November 26th, 2026

DOI: https://doi.org/10.21203/rs.3.rs-11796758/v1

License: This work is licensed under a Creative Commons Attribution 4.0 International License.
Read Full License

Additional Declarations: No competing interests reported.

Abstract

Carbon fiber reinforced thermoplastic composites (CFRTCs) are attractive for lightweight structures because of their high specific strength and stiffness, but in humid environments they absorb water and lose part of their load-bearing capacity. Short carbon fiber (SCF) was oxidized in concentrated nitric acid (65–68 wt%) for 6 h, and SCF/ABS composites containing 0, 5, 10, 20 and 30 wt% fiber were prepared by twin-screw extrusion followed by micro-injection molding. The mechanical properties, water absorption behavior and fracture morphology of the composites were compared after water saturation. At 20 wt% fiber content the tensile strength increased from 51.8 MPa for pure ABS to 72.6 MPa for the unmodified and 85.7 MPa for the modified composite, the yield strength from 41.3 to 64.4 and 69.5 MPa, and the impact strength from 3.92 to 4.39 and 4.69 kJ/m^2, while at 30 wt% fiber the elongation at break fell from 8.04% to 2.61% (unmodified) and 1.97% (modified). The equilibrium water uptake decreased with increasing fiber content, from 0.81% for pure ABS to 0.68% for the unmodified and 0.60% for the modified composite at 30 wt%, and at a given fiber content the modified composites absorbed 9.6–11.8% less water than the unmodified ones. Water saturation reduced the mechanical properties of every composition: for the modified 20 wt% composite the tensile strength decreased from 85.7 to 52.8 MPa and the impact strength from 4.69 to 4.25 kJ/m^2. Nitric acid oxidation of SCF is an effective route to stronger SCF/ABS composites at the cost of ductility.

1. Introduction

Plastics are used in almost every aspect of daily life, and the demand for lightweight structural materials has grown steadily as a way of reducing energy consumption [1]. Carbon fiber (CF) combines high specific strength and stiffness with low density and good toughness, and it is produced on a large scale; carbon fiber reinforced thermoplastic composites (CFRTCs) are therefore expected to become one of the most important classes of lightweight materials [2].

CF has already replaced steel and other metals in many applications. For example, CFRTCs are used in lightweight bone structures and in the sensing–actuation units of humanoid robots [3], and they have become irreplaceable in a number of fields [4–6] because the properties of carbon fiber reinforced polymers can be tailored over a wide range. The manufacturing routes developed so far, however, share a common bottleneck: the compatibility between the polymer matrix and the CF. The CF surface is smooth and carries few active groups, i.e., it is physically and chemically inert, so that the fiber is poorly wetted by the polymer melt and the interfacial adhesion is weak. Surface treatment of the CF is therefore the key to improving the mechanical properties of CF-reinforced polymers [7]. Chukov et al. [8] used polysulfone (PSU) as the matrix and oxidized the CF at 500°C for 30 min in order to improve the fiber–PSU bonding; compared with the untreated composite, the tensile and bending strengths increased from 880 and 899 MPa to 1047 and 1042 MPa, i.e., by 18.98% and 15.91%, respectively. Tian et al. [9] oxidized CF in concentrated HNO_3 for 0, 30, 60, 90 and 120 min and found that HNO_3 oxidation introduces polar groups onto the fiber surface more efficiently than other routes and thereby improves the wettability of the fiber. Compared with the untreated CF/polypropylene composite, the composite containing CF

oxidized for 90 min showed the best mechanical properties, its tensile and impact strengths increasing by 35.91% and 54.97%, respectively. Zhang and Ding [10] treated CF electrochemically in HNO_3 for 1 h at a current of 150 mA and reported a pronounced increase both in the surface roughness of the fiber and in the disorder of its surface carbon atoms. With the aim of improving the CF/polycarbonate interface, Liu et al. [11] sized CF with water-borne polycarbonate and polyurethane sizing agents containing carbon nanotubes; at a nanotube content of 0.1 wt% the interfacial shear strength reached its maximum, and the tensile strengths of the polyurethane- and polycarbonate-sized composites increased by 97.6% and 87.93%, respectively. Lu et al. [12] treated CF by short-shot plasma and found that the surface roughness increased appreciably and that the interlaminar shear strength of the composite reached 59.73 MPa, i.e., 41.01% higher than that of the untreated composite.

Research on SCF-reinforced composites has so far concentrated on their mechanical properties. Garcia et al. [13] studied the impact behavior of SCF-reinforced poly(ether ether ketone) composites and found that the addition of SCF increases the strength and the stiffness but reduces the ductility and the impact strength. Chukov et al. [14] prepared CF-reinforced ultra-high molecular weight polyethylene composites and showed that the interfacial interaction between the polyethylene matrix and the CF is greatly enhanced after high-temperature thermal oxidation of the fiber. Rezaei et al. [15] investigated SCF-reinforced polypropylene composites and found that the thermomechanical properties and the damping performance improve as the fiber length increases. Fu et al. [16] studied in detail the tensile properties of injection-molded short glass fiber and SCF reinforced polypropylene and showed that these properties are governed by the combined effect of the fiber volume fraction and the fiber length. Karsli and Aytac [17] prepared CF-reinforced polyamide 6 composites by melt mixing and found that increasing the fiber content increases the tensile strength, the modulus and the hardness but decreases the fracture strain. Ameli et al. [18] studied the foaming behavior and the through-plane electrical conductivity of low-pressure injection-molded polypropylene/CF composites and showed that a high conductivity of the foam is obtained when the fiber orientation in the plane of the sheet is increased and the thickness of the surface layer is reduced. Solomon et al. [19] prepared short glass fiber/SCF hybrid-fiber-reinforced polyamide 6 composites and obtained the highest impact strength and impact energy for the sandwich-structured CF-skin/glass-fiber-core composites. Unterweger et al. [20] prepared SCF/polypropylene composites from plasma-treated CF and found that the mechanical properties are closely related to the interfacial properties of the fiber. Run et al. [21] investigated poly(trimethylene terephthalate)/ABS/SCF composites and showed that at an ABS content of 5 wt% the SCF significantly increases the tensile and flexural strengths. Lopes and d'Almeida [22] analyzed the effect of CF reinforcement in neat ABS and reported increases of up to 38% in tensile strength and 90% in modulus relative to neat ABS. Ajinjeru et al. [23] studied the dynamic rheological properties of 20 wt% CF/ABS, 25 wt% CF/polyphenylsulfone, 35 wt% CF/polyethersulfone and 40 wt% CF/polyphenylene sulfide and found that the 20 wt% CF/ABS and the 40 wt% CF/polyphenylene sulfide melts show a dominant elastic component and strong shear thinning over the whole frequency range. The same group [24] showed that the viscosity of unreinforced ABS decreases by more than 50% with increasing temperature, whereas the addition of 20 wt% CF

increases it more than fourfold, which indicates that the fiber content that can be processed is limited by the melt viscosity.

Short-fiber and particle reinforcements have also been examined in other matrices: nanocellulose in PVDF membranes [25], chopped CF in ZrB_2–SiC ceramics [26], CF fabrics for resin transfer molding [27] and carbon black in PA6/HDPE [28], although these studies address properties other than the interfacial and moisture behavior considered here. For ABS specifically, Ahmad et al. [29] analyzed the water absorption of oil palm fiber-reinforced ABS composites containing 0, 3, 5 and 7 wt% fiber, produced by fused deposition modeling, and showed that the uptake increases with the fiber content, a trend opposite to that found here for the hydrophobic carbon fiber and one that reflects the hydrophilic nature of the oil palm fiber. Only a limited number of studies address ABS-based composites, although ABS is one of the most widely used amorphous thermoplastics for injection-molded parts. Çavdar et al. [30] examined nanocellulose-reinforced ABS nanocomposites and showed that the filler changes the mechanical, thermal and morphological behavior simultaneously, so that no single property can be used to judge the efficiency of a filler. Karagöz et al. [31] compared ABS composites reinforced with bentonite and with DEHPA-modified bentonite and found that the surface modification improves some properties while leaving others unchanged or even deteriorating them, which shows that a treatment does not necessarily shift all the properties in the same direction. Lapčík et al. [32] reviewed ABS nanocomposites for technical and biomedical applications and emphasized that the filler content, the morphology and the statistical reliability of the data must be reported together if results from different studies are to be compared. Sepetcioglu et al. [33] showed for a basalt fiber/epoxy system that hydrothermal aging progressively reduces the mechanical properties and that the retention depends on the aging time, which is directly relevant to the interpretation of the water absorption data of short-fiber composites. Finally, Sepet et al. [34] showed for particle-filled HDPE that the tensile, impact and creep behavior must be considered together, because the short-term properties that are usually reported are not sufficient to qualify a material for engineering use. These observations define the framework of the present work: the effect of the nitric acid treatment has to be evaluated at a constant fiber content, in the dry and in the wet state, and the gain in strength has to be discussed together with the loss of ductility and with the reduction in water uptake.

The novelty of the present work is therefore threefold. First, the effect of nitric acid oxidation is evaluated at a constant fiber content for a single ABS matrix over a wide composition range (0–30 wt%), so that the change produced by the treatment is separated from that produced by the fiber content. Second, the mechanical properties are measured both before and after water saturation, which makes it possible to determine whether the improved interfacial adhesion also reduces the loss of properties caused by moisture. Third, the water uptake is analyzed in terms of the parameters of Fickian diffusion, so that the treatment is judged not only by the strength but also by the moisture resistance. Nitric acid oxidation was selected because it is known to introduce carbonyl, carboxyl and hydroxyl groups onto the CF surface and to etch the fiber, thereby increasing its surface roughness [9, 10, 12]; both effects are expected to favor the wetting of the fiber by the ABS melt and to promote hydrogen bonding and dipole interactions between the oxygenated fiber surface and the polar acrylonitrile segments of ABS. The

same oxidation, however, increases the polarity of the fiber surface, which may in principle increase its affinity for water; the net effect on the water uptake is therefore not obvious, and it is one of the points examined below. Accordingly, SCF/ABS composites were prepared with unmodified and with nitric acid-modified fiber, and the influence of water absorption on their mechanical properties was studied. The results are intended as a reference for assessing the durability of these composites in humid environments.

2. Materials and methods

2.1. Materials

The main raw materials were ABS (PA-757K, Jiangsu Zhenjiang Qimei Chemical Co., Ltd., China) and SCF (CJ-CF300, Cangzhou Zhongli New Material Technology Co., Ltd., China). The fibers were 6 mm long and 6.9 μm in diameter, and their density was 1800 kg/m^3. The nitric acid used for the surface modification was a 65–68 wt% aqueous solution (China National Pharmaceutical Group Chemical Reagent Co., Ltd., China).

2.2. Equipment and instruments

The following equipment was used: a mixer (GRS77-11.98M1, Guangdong Lina Industrial Co., Ltd., China), a crusher (ECY250, Dongguan Huiying Plastic Machinery Co., Ltd., China), a twin-screw extruder (BP-8177-Z, Dongguan Baopin Precision Instrument Co., Ltd., China), a vacuum drying oven (KL-DHG-9070-A, Kunlun Testing Instrument Co., Ltd., China), an electronic balance (CP214, Ohaus Instrument (Changzhou) Co., Ltd., USA), a micro-injection molding machine (BOY-XS, BOY Co., Germany), a mold temperature controller (TP6ZE, Piwang Co., China) and a chiller (ML-CA03, Shanghai Yinguan Electromechanical Equipment Co., Ltd., China).

2.3. Specimen preparation

The SCF was oxidized in nitric acid (65–68 wt%) at 120°C under reflux for 6 h, using 30 mL of acid per gram of fiber; residual acid was then removed by washing with deionized water until the washings were neutral, and the fiber was dried in a vacuum oven (120°C for 2 h). The ABS pellets and both the modified and the unmodified SCF were dried at 80°C for 5 h in a vacuum oven. The SCF and the ABS pellets were mixed for 0.5 h in the proportions given in Table 1, crushed, and extruded and pelletized in the twin-screw extruder; the pellets were dried again before molding. Table 1 lists the mass fractions of the compositions studied; because pure ABS is common to both series, nine distinct compositions were investigated in total. Fiber contents of 0, 5, 10, 20 and 30 wt% were chosen because they span the range from dilute to highly filled short-fiber thermoplastic composites reported in the literature [16, 17, 22], 30 wt% being the highest content that could still be processed reproducibly in the injection molding machine used here.

Table 1
Mass Fractions of Carbon Fiber Reinforced ABS Composites.

ID	Unmodified CF/wt%	ABS/wt%	ID	Modified CF/wt%	ABS/wt%
1	0	100	1	0	100
2	5	95	6	5	95
3	10	90	7	10	90
4	20	80	8	20	80
5	30	70	9	30	70

The barrel of the twin-screw extruder was preheated for 30–60 min until the temperature had stabilized; the six zones were set to 220, 230, 230, 230, 240 and 240°C, the screw speed was 30 rpm and the feeding rate 20 rpm. The nine compositions were extruded and pelletized, dried at 80°C for 5 h and injection molded under the conditions listed in Table 2. Ten specimens were molded for each composition and five were used for each test; the specimen geometry is shown in Fig. 1. The complete preparation and testing procedure is summarized in Fig. 2.

Table 2
Injection Molding Process Parameters.

Melt temperature / °C	Mold temperature / °C	Holding pressure /MPa	Injection pressure /MPa	Cooling time /s	Injection time /s
220	50	60	80	5	1

2.4. Characterization

Tensile properties and elongation at break were determined on dumbbell-shaped specimens (Fig. 1) in accordance with GB/T 1040.2–2022. The tensile speed was 50 mm/min. Five specimens were tested for each composition. The mechanical properties are reported as the mean of five specimens, and the water-absorption data as the mean ± standard deviation of five specimens.

Unnotched impact specimens of rectangular cross-section were tested in accordance with GB/T 1843–2008 (instrumented Izod test). Five specimens of each composition were tested. The impact strength is expressed per unit cross-sectional area (kJ/m^2), and all the values reported below are expressed in this unit.

Water absorption was measured on five specimens of each composition. The specimens were dried to constant mass, weighed and immersed in deionized water at 23°C in accordance with ASTM D570 and ASTM D5229/D5229M. At specified intervals the specimens were removed, the surface water was blotted off and the mass was recorded. The measurements were continued for one month, which was long enough for the uptake curves to reach a plateau.

Fracture surfaces were examined with an optical metallographic microscope (Axio Vert A1) at a magnification of 200× in order to assess the dispersion of the SCF in the ABS matrix at different fiber contents and the adhesion between fiber and matrix after fracture. Optical microscopy resolves only the mesoscale morphology; the chemical state of the interface and the fine structure of the fiber surface were not characterized in this work.

3. Results and discussion

3.1. Comparison of mechanical properties

Figure 3(a) shows that the elongation at break decreased with increasing CF content. At the same fiber content it was lower for the modified composite, the highest value (8.04%) being that of pure ABS. At 30 wt% CF the elongation at break was 1.97% for the modified and 2.61% for the unmodified composite; at 5 wt% CF it had already fallen sharply, by 49.7% for the modified and by 35.1% for the unmodified composite, relative to pure ABS. Figure 3(b) shows that the impact strength first increased and then decreased with increasing CF content and was higher for the modified composite at every fiber content. The impact strength of pure ABS was the lowest (3.92 kJ/m^2); it was highest at 20 wt% CF, where the unmodified and the modified composites reached 4.39 and 4.69 kJ/m^2, i.e., 12.0% and 19.6% more than pure ABS. At 30 wt% CF it decreased again, because the excess fiber increased the brittleness of the composite [35]. Figure 3(c) shows that the tensile strength increased gradually up to 20 wt% CF and then decreased sharply, and that it was higher for the modified composite. The tensile strength of pure ABS was the lowest (51.8 MPa), and the highest values were obtained at 20 wt% CF: 72.6 MPa for the unmodified and 85.7 MPa for the modified composite, i.e., 40.2% and 65.4% more than pure ABS.

Figure 3(d) shows that the yield strength followed the same trend. It was higher for the modified composite at every fiber content, reaching 69.5 MPa against 64.4 MPa at 20 wt% CF, while that of pure ABS was the lowest (41.3 MPa); the values obtained at 20 wt% CF were thus 55.9% and 68.3% higher than that of pure ABS for the unmodified and the modified composite, respectively. At 30 wt% CF the yield strength of the modified and of the unmodified composite decreased by 32.3% and 29.7%, respectively, relative to the 20 wt% values. An excessive CF content thus leads to uneven dispersion and to agglomeration of the fibers in the matrix and hence to stress concentration [36], so that the mechanical properties decrease sharply.

It should be stressed that 20 wt% is the optimum of the compositions tested rather than a proven optimum, because no compositions between 10 and 20 wt% or between 20 and 30 wt% were prepared. The increase in strength is also accompanied by a loss of ductility: over the whole composition range the elongation at break decreased while the strength increased, and the modified composites, which are the strongest, are also the least ductile. This strength–toughness trade-off has been reported for other short-fiber systems [13, 17, 22] and is typical of an improvement in interfacial adhesion, which suppresses fiber pull-out and the associated energy dissipation. The elastic modulus was not determined in this work, so that the increase in stiffness that usually accompanies an increase in fiber

content could not be quantified; for the same reason, no quantitative claim about the stiffness of these composites is made below.

In summary, the addition of SCF markedly improved the tensile, yield and impact strengths of the ABS matrix. Up to 20 wt% CF all three properties increased with the fiber content, which indicates that the reinforcement is effective over this range; above 20 wt% they decreased again because of agglomeration. At a given fiber content the mechanical properties of the modified composite were higher than those of the unmodified one, which indicates that the modified CF is more compatible with the ABS matrix and that the interfacial bonding is stronger. With increasing CF content, however, the toughness of the composite decreased considerably, and the elongation at break decreased monotonically.

3.2. Comparison of mechanical properties before and after water absorption

In humid environments CFRTCs absorb water, which degrades their performance. Figure 4(a) shows the maximum force–deformation curves of the unmodified composites before and after water absorption; they reflect the brittleness, plasticity, yield and fracture behavior in the dry and in the wet state. For the composites, the maximum force in the dry state was higher than that after absorption. For pure ABS the maximum force after immersion was 258.9 N and the deformation 2.39 mm; relative to the dry specimen the deformation decreased by 36.8%, whereas the maximum force changed by only 3.8% (from 249.4 to 258.9 N), which is within the scatter of the measurement.

For the composites, both the maximum force and the deformation at which it was reached decreased after absorption (Fig. 4(a, b)), i.e., the materials became more brittle; pure ABS was the only exception, its maximum force remaining essentially unchanged. Water molecules penetrate the matrix and increase the distance between the polymer chains, which causes swelling; the osmotic pressure of the absorbed water nucleates new cracks, and the growth of these cracks in turn increases the water uptake. Cracks that open along the fibers also cause debonding between the CF and the matrix, which markedly reduces the mechanical properties. Water absorption therefore not only lowers the mechanical properties but also changes the dimensions of the specimen. After absorption the maximum force of the 20 wt% CF composite decreased by 43.1% for the unmodified and by 36.9% for the modified composite, while the deformation at maximum force decreased by more than 30% in both cases (Fig. 4). Note that the forces plotted in Fig. 4 are not normalized by the cross-section of the specimen, so the sequence of the force maxima need not follow that of the tensile strengths of Fig. 3(c); what is compared here is the dry and the saturated state of the same specimens.

Figure 7. Comparison of tensile strength of modified and unmodified composites before and after water absorption: (a) Unmodified CF, (b) Modified CF.

Figure 7 shows that the tensile strength of all the materials decreased after water absorption: from 51.8 to 43.8 MPa (by 15.4%) for pure ABS, from 72.6 to 46.6 MPa for the unmodified and from 85.7 to 52.8 MPa for the modified composite. Figure 8 shows that the yield strength decreased as well: from 41.3 to

40.2 MPa (by 2.7%) for pure ABS, from 64.4 to 44.3 MPa (by 31.2%) for the unmodified and from 69.5 to 45.8 MPa (by 34.1%) for the modified composite. The modified composite thus lost a slightly larger fraction of its strength than the unmodified one, so that the advantage gained by the modification is partly, but not completely, lost after saturation: in the saturated state the tensile strength of the modified composite (52.8 MPa) is still 13.3% higher than that of the unmodified one (46.6 MPa). Expressed as retention, the modified composites retained 61.6% of their tensile strength, 65.9% of their yield strength and 90.6% of their impact strength, against 64.2%, 68.8% and 98.2% for the unmodified ones, so that the modification raised the absolute level of the properties in the wet state without improving the fraction retained.

3.3. Water absorption kinetics of composites

The durability of a composite in a humid environment is governed by its water uptake, which eventually degrades the mechanical properties [37]; an understanding of the absorption mechanism is therefore essential for predicting the service performance of the material. Water absorption accelerates the degradation of the fiber–matrix interface, which in turn reduces the mechanical properties and changes the dimensions of the composite [38–42]. The water uptake was determined in accordance with ASTM D570 and calculated from Eq. (1) [43, 44].

$$W_t = \frac{M_t - M_0}{M_0} \times 100\%$$

1

where M_0 and M_t are the masses of the dry specimen and of the specimen at time t, respectively.

The models used to describe the water absorption behavior of composites follow from Fick's law of diffusion. The diffusion, adsorption and permeability coefficients were therefore calculated from the Fickian relations given by Eqs. (2)–(5) [42, 43, 45], and the intercept and the slope of the water absorption curves, which are used to identify the type of diffusion [39, 46], are defined by Eqs. (6) and (7).

$$N = \pi \frac{h^2 m^2}{16 W_s^2}$$

2

$$N_c = N\left(1 + \frac{h}{l} + \frac{h}{b}\right)^{-2}$$

3

$$Q = \frac{W_s}{W_{max}}$$

4

$$P = N_c \cdot Q$$

5

where N_c is the corrected diffusion coefficient (N is the diffusion coefficient of an infinite plate), $m = \frac{W_{t2} - W_{t1}}{\sqrt{t_2} - \sqrt{t_1}}$ is the slope of the initial linear part of the sorption curve plotted against √t, h is the initial thickness of the specimen (mm), and l and b are the length and the width of the specimen. W_s is the equilibrium (saturation) water uptake and W_{max} is the maximum water-absorption capacity of the material, so that the adsorption (solubility) coefficient $Q = W_s/W_{max}$ is dimensionless ($0 < Q < 1$) and represents the fraction of the sorption capacity of the composite that is occupied by water; $P = Q \cdot N_c$ is the permeability coefficient, which combines the solubility and the diffusivity of water in the composite.

$$\frac{W_t}{W_s} = kt^n$$

6

$$log\left(\frac{W_t}{W_s}\right) = log\, k + n\, log\, t$$

7

where t is the time, W_t is the water uptake at time t, k is the constant of the interaction between the composite specimen and water, and n is the constant of the diffusion mode.

The rate of water uptake governs both the mechanical properties and the dimensional stability of a composite. Water penetrates a composite mainly by diffusion, which depends on the mobility of the water molecules in the micro-gaps between polymer chain segments. Two mechanisms dominate: (i) flow of water along the capillaries of the fiber–matrix interface, which becomes important when the adhesion at this interface is poor or when the interface starts to debond, and (ii) formation of micro-cracks by swelling of the matrix around the fibers, in which water can flow and be stored. The experimental uptake curves are plotted against the square root of time in Fig. 9. Pure ABS showed the highest uptake of all the materials studied, and the uptake decreased as the CF content increased, because the hydrophobic CF acts as a barrier to water. At a given fiber content the unmodified composites absorbed more water than the modified ones. Each data point is the mean of five specimens, and the error bars represent the standard deviation (n = 5). The curves show the characteristic shape of Fickian diffusion [47–49]: a linear increase at short times followed by a plateau. The equilibrium water uptake of the composites is listed in Table 3.

Table 3
Equilibrium Water Uptake of the Composites. (Values are means ± SD (n = 5)).

Unmodified CF		**Modified CF**	
Materials	Water uptake/%	Materials	Water uptake/%
ABS	0.81 ± 0.008	ABS	0.81 ± 0.008
5 wt% CF	0.77 ± 0.007	5 wt% CF	0.69 ± 0.006
10 wt% CF	0.73 ± 0.006	10 wt% CF	0.66 ± 0.005
20 wt% CF	0.69 ± 0.004	20 wt% CF	0.61 ± 0.003
30 wt% CF	0.68 ± 0.005	30 wt% CF	0.60 ± 0.004

The hydrophobic character of CF reduces the water uptake, so that a higher fiber content leads to a lower uptake: the fibers act as a barrier and reduce the absorption capacity of the material. As shown in Table 3, the equilibrium uptake of the modified composites was lower than that of the unmodified ones at every fiber content, the reduction being 9.6–11.8% (e.g. from 0.68% to 0.60% at 30 wt% CF). This indicates that the nitric acid modification improved the interfacial adhesion between the polymer matrix and the fiber surface and reduced the free volume and the interfacial voids available for water storage. Depending on the relative importance of the penetrant mobility and of the relaxation of the polymer chains, diffusion is usually classified into three types: (i) $n = 0.5$, Fickian (case I) diffusion, in which the diffusion of water is much slower than the relaxation of the polymer chains; (ii) $n = 1$, case II diffusion, in which diffusion is much faster than relaxation; and (iii) $0.5 < n < 1$, anomalous diffusion, in which the mobility of the water molecules is comparable to that of the chain segments. The coefficients k and n were obtained by linear regression of the experimental data and are listed in Table 4; the values of n lie between 0.116 and 0.221, i.e., well below 0.5. Because the initial uptake of a thin sheet should follow $n \approx 0.5$ for ideal Fickian diffusion, these low exponents cannot by themselves be taken as proof of Fickian behavior; they indicate that much of the initial uptake occurred before the first weighing, so that the early stage of the process was not resolved by the measuring schedule. The classification adopted here therefore rests on the shape of the complete curves (Fig. 9), which show a linear initial region followed by a well-defined plateau, as expected for Fickian diffusion. A rigorous verification would require a comparison of the experimental curves with the complete series solution of Fick's second law for the actual specimen geometry; this was not attempted here, and the classification should be regarded as tentative.

Table 4
Kinetic Parameters of Water Absorption. (Values are means ± SD (n = 5)).

Unmodified CF			**Modified CF**		
Materials	*n*	*k*	Materials	*n*	*k*
ABS	0.144 ± 0.004	0.351 ± 0.012	ABS	0.144 ± 0.004	0.351 ± 0.012
5 wt% CF	0.131 ± 0.004	0.376 ± 0.011	5 wt% CF	0.143 ± 0.003	0.351 ± 0.010
10 wt% CF	0.116 ± 0.003	0.407 ± 0.009	10 wt% CF	0.137 ± 0.002	0.382 ± 0.008
20 wt% CF	0.145 ± 0.002	0.375 ± 0.008	20 wt% CF	0.159 ± 0.001	0.327 ± 0.005
30 wt% CF	0.169 ± 0.003	0.292 ± 0.007	30 wt% CF	0.221 ± 0.002	0.207 ± 0.006

The diffusion, adsorption and permeability coefficients of the modified and of the unmodified composites are compared in Table 5. The adsorption, permeability and diffusion coefficients of the modified composites were all lower than those of the unmodified ones at every nonzero fiber content. Above 5 wt% CF the diffusion and permeability coefficients decreased with increasing fiber content, and the adsorption coefficient decreased as well apart from the 10 wt% composition, which is slightly above the 5 wt% one. Together with the data of Tables 3 and 4, this confirms that the modified composite absorbs less water than the unmodified one at the same fiber content; the difference is, however, moderate, and it is largest at the highest fiber contents, where the interface controls the uptake.

Table 5
Diffusion, Adsorption and Permeability Coefficients of the Composites. (Values are means ± SD (n = 5); Q is dimensionless, and N_c and P are expressed in 10^{-6} mm²/s)).

Unmodified CF				**Modified CF**			
Materials	Q	N_c	P	Materials	Q	N_c	P
ABS	0.65 ± 0.005	4.99 ± 0.12	3.25 ± 0.08	ABS	0.65 ± 0.005	4.99 ± 0.12	3.25 ± 0.08
5 wt% CF	0.65 ± 0.004	5.14 ± 0.11	3.32 ± 0.07	5 wt% CF	0.64 ± 0.005	4.27 ± 0.11	2.73 ± 0.07
10 wt% CF	0.68 ± 0.004	4.53 ± 0.11	3.09 ± 0.08	10 wt% CF	0.65 ± 0.006	4.16 ± 0.09	2.71 ± 0.06
20 wt% CF	0.65 ± 0.003	4.01 ± 0.08	2.61 ± 0.05	20 wt% CF	0.58 ± 0.002	3.79 ± 0.07	2.19 ± 0.04
30 wt% CF	0.59 ± 0.003	3.83 ± 0.09	2.25 ± 0.05	30 wt% CF	0.48 ± 0.004	3.48 ± 0.08	1.68 ± 0.04

3.4. Cross-section morphology of composites

Figures 10 and 11 show that the dispersion of the CF in the ABS matrix deteriorated as the fiber content increased, agglomeration becoming evident at 20 and 30 wt% CF. At 5 and 10 wt% CF the fibers were dispersed relatively uniformly, and the tensile and yield strengths increased with the fiber content. At 20 wt% CF isolated agglomerates appeared although the strength still reached its maximum, which suggests that at this content the reinforcing effect of the fiber still outweighed the damage caused by the inhomogeneity. At 30 wt% CF the agglomerates were large and numerous and the matrix between them was no longer continuous, so that the tensile, yield and impact strengths decreased sharply and the material became brittle. A large number of fibers were pulled out of the unmodified composites, which indicates poor interfacial compatibility between the unmodified CF and the matrix and explains why their mechanical properties were lower than those of the modified ones.

3.5. Mechanism of interfacial modification and moisture resistance

The results of Sections 3.1–3.4 can be explained by the interfacial mechanism shown schematically in Fig. 12. Nitric acid oxidation introduces carboxyl, hydroxyl and carbonyl groups onto the SCF surface and etches the fiber, so that its roughness and specific surface area increase [9, 10, 12]. In the unmodified composites the smooth and chemically inert surface is poorly wetted by the ABS melt, and interfacial voids remain after molding (Fig. 12(a)); these voids store water, provide continuous paths for capillary transport along the interface, and act as initiation sites for debonding, which is consistent with the extensive fiber pull-out seen in Fig. 10. In the modified composites the oxygenated and roughened surface is wetted more readily, hydrogen bonds and dipole interactions can form between the oxygen-containing groups on the fiber and the polar nitrile groups of the acrylonitrile segments, and the melt penetrates the etched surface and interlocks with it mechanically (Fig. 12(b)). The denser interface transfers load to the fiber more efficiently, which raises the tensile, yield and impact strengths, but it also suppresses pull-out and the associated plastic deformation, which explains the lower elongation at break of the modified composites. The same densification reduces the free volume and the interfacial voids available for water, so that the equilibrium uptake and the diffusion, adsorption and permeability coefficients are all lower for the modified composites (Tables 3 and 5).

Figure 13 collects the equilibrium water uptake of the two series and shows both trends together: the uptake falls as the fiber content increases, and the modified composite lies below the unmodified one at every fiber content. Taken together, Figs. 12 and 13 make the practical significance of the treatment explicit: nitric acid oxidation raises the strength of SCF/ABS composites both before and after water saturation and at the same time lowers their equilibrium water uptake, the largest combined benefit being obtained at 20 wt% CF, where the modified composite combines the highest strengths of the series with a water uptake 11.6% lower than that of the unmodified composite.

4. Conclusions

In this work the mechanical properties, the water absorption behavior and the fracture morphology of SCF/ABS composites containing unmodified and nitric acid-modified short carbon fibers were studied over the 0–30 wt% fiber range. Within this range, the highest tensile, yield and impact strengths of both series were obtained at 20 wt% CF, which is the optimum of the compositions tested rather than a proven optimum. At 20 wt% the nitric acid modification increased the tensile strength from 72.6 to 85.7 MPa, the yield strength from 64.4 to 69.5 MPa and the impact strength from 4.39 to 4.69 kJ/m^2, while the elongation at break decreased; relative to pure ABS, the tensile, yield and impact strengths of the modified 20 wt% composite were higher by 65.4%, 68.3% and 19.6%, respectively. The equilibrium water uptake decreased with increasing fiber content, from 0.81% for pure ABS to 0.68% (unmodified) and 0.60% (modified) at 30 wt%, and at a given fiber content the modified composites absorbed 9.6–11.8% less water than the unmodified ones. Water saturation reduced the mechanical properties of every composition; for the modified 20 wt% composite the tensile strength decreased from 85.7 to 52.8 MPa, the yield strength from 69.5 to 45.8 MPa and the impact strength from 4.69 to 4.25 kJ/m^2, and the deformation at maximum force decreased by more than 30%. Nitric acid oxidation of SCF is therefore an effective way of raising the strength of SCF/ABS composites and of limiting their moisture uptake, at the cost of a loss of ductility. The mechanism behind this improvement is summarized in Fig. 12: a denser and chemically bonded interface transfers load more efficiently and leaves less free volume for water storage. Because the surface chemistry, the fiber length distribution, the elastic modulus and the thermal properties were not characterized in this work, the trends reported here should be confirmed by further experiments, including FTIR/XPS analysis of the fiber surface, SEM of the fracture surfaces and dynamic mechanical analysis, before these materials are considered for specific load-bearing applications.

Declarations

Competing interests.

The authors have no relevant financial or non-financial interests to disclose.

Funding.

This work was supported by Tianjin Science and Technology Plan Project, China (Grant number 25YFYFFG00100).

Availability of data and materials. The data that support the findings of this study are available from the corresponding author on reasonable request.

Ethics, Consent to Participate, and Consent to Publish declarations: Not applicable.

Author Contribution

Lixiang He: writing – original draft. Quan Wang: writing – review and editing. Tuo Cheng: data curation. Qun Zhang: methodology.

References

1. Dehghan-Banadaki Z., Ahmadi M.S. and Mashroteh H., “Experimental and Theoretical Investigation of the Tensile Properties of Green Poly(Lactic Acid) Composites Reinforced with Date Palm Fibers,” Mech. Compos. Mater., 62, No. 2, 213–230(2026).
2. Nobe R., Qiu J.H., Kudo M. and Zhang G.H., “Morphology and mechanical investigation of microcellular injection molded carbon fiber reinforced polypropylene composite foams,” Polym. Eng. Sci., 60, No. 7, 1507–1519(2020).
3. Zhu G.Y., Liu C.Y., Deng B., Liu B.E., Xia P.C., Li P.J., Lei J. and Xu J.Z., “Research progress in polymers for humanoid robots,” Acta Polym. Sin., 57, No. 7, 1433–1445(2026).
4. Palmer J., Savage L., Ghita O.R. and Evans K.E., “Sheet moulding compound (SMC) from carbon fibre recyclate,” Compos. Part A-Appl. Sci. Manuf., 41, 1232–1237(2010).
5. Magniez K., Iftikhar R. and Fox B.L., “Properties of bio-based polymer Nylon 11 reinforced with short carbon fiber composites,” Polym. Compos., 36, No. 4, 668–674(2015).
6. Nash N.H., Young T.M. and McGrail P.T., “Inclusion of a thermoplastic phase to improve impact and post-impact performances of carbon fibre reinforced thermosetting composites-a review,” Mater. Des., 85, 582–597(2015).
7. Ma Z.Y., Qian Z. and Cai J.B., “Effects of manufacturing process and surface treatments on mechanical properties of PLA/SCF composites using extrusion printing,” J. Mech. Sci. Technol., 36, No. 5, 2355–2367(2022).
8. Chukov D.I., Nematulloev S.G., Tcherdyntsev V.V., Torokhov V.G., Stepashkin A.A., Zadorozhnyy M.Y., Zherebtsov D.D. and Sherif G., “Structure and properties of polysulfone filled with modified twill weave carbon fabrics,” Polymers, 12, No. 1, 50(2020).
9. Tian H.F., Yao Y.Y., Liu D., Li Y.C., Jv R., Xiang G. and Xiang A.M., “Enhanced interfacial adhesion and properties of polypropylene/carbon fiber composites by fiber surface oxidation in presence of a compatibilizer,” Polym. Compos., 40, No. S1, 654–662(2019).
10. Zhang S. and Ding Q., “The surface modification of carbon fiber for thermoplastic HDPE composites,” Surf. Interface Anal., 51, No. 2, 184–189(2018).
11. Liu Y.T., Li L., Wang J.P., Fei Y.J., Liu N.D. and Wu G.P., “Effect of carbon nanotube addition in two sizing agents on interfacial properties of carbon fiber/polycarbonate composites,” New Carbon Mater., 36, 639–648(2021).
12. Lu C.R., Qiu S., Wang J., Wang J., Xiao L., Zheng T., Wang X.D. and Zhang D.X., “Enhancing the interfacial strength of carbon fiber/poly(ether ether ketone) hybrid composites by plasma treatments,” Polymers, 11, No. 5, 753(2019).

13. Garcia G.D., Rodriguez M.M., Rusinek A. and Arias A., “Investigation of mechanical impact behavior of short carbon-fiber-reinforced PEEK composites,” Compos. Struct., 133, 1116–1126(2015).
14. Chukov D.I., Stepashkin A.A., Maksimkin A.V., Tcherdyntsev V.V., Kaloshkin S.D., Kuskov K.V. and Bugakov V.I., “Investigation of structure, mechanical and tribological properties of short carbon fiber reinforced UHMWPE-matrix composites,” Compos. Part B-Eng., 76, 79–88(2015).
15. Rezaei F., Yunus R., Ibrahim N.A. and Mahdi E.S., “Development of short-carbon-fiber-reinforced polypropylene composite for car bonnet,” Polym.-Plast. Technol. Eng., 47, No. 4, 351–357(2008).
16. Fu S.Y., Lauke B., Mader E., Yue C.Y. and Hu X., “Tensile properties of short-glass-fiber-and short-carbon-fiber-reinforced polypropylene composites,” Compos. Part A-Appl. Sci. Manuf., 31, 1117–1125(2000).
17. Karsli N.G. and Aytac A., “Tensile and thermomechanical properties of short carbon fiber reinforced polyamide 6 composites,” Compos. Part B-Eng., 51, 270–275(2013).
18. Ameli A., Jung P.U. and Park C.B., “Through-plane electrical conductivity of injection-molded polypropylene/carbon-fiber composite foams,” Compos. Sci. Technol., 76, 37–44(2013).
19. Solomon S., Bakar A.A., Ishak Z.A., Leong Y.W., Ishiaku U.S. and Hamada H., “Drop weight impact properties of (CO) injection molded short glass fiber/short carbon fiber/polyamide 6 hybrid composites,” J. Reinf. Plast. Compos., 26, 405–418(2007).
20. Unterweger C., Duchoslav J., Stifter D. and Fürst C., “Characterization of carbon fiber surfaces and their impact on the mechanical properties of short carbon fiber reinforced polypropylene composites,” Compos. Sci. Technol., 108, 41–47(2015).
21. Run M.T., Wang H.S. and Li X., “Morphology, mechanical, rheological, and thermal properties study on the PTT/ABS/SCF composites,” Compos. Interfaces, 19, No. 5, 333–351(2012).
22. Lopes B.J. and d'Almeida J.R.M., “Initial development and characterization of carbon fiber reinforced ABS for future additive manufacturing applications,” Mater. Today-Proc., 8, 719–730 (2019).
23. Ajinjeru C., Kishore V., Chen X., Hershey C., Lindahl J., Kunc V., Hassen A.A. and Duty C., “Rheological survey of carbon fiber-reinforced high-temperature thermoplastics for big area additive manufacturing tooling applications,” J. Thermoplast. Compos. Mater., 34, No. 11, 1443–1461(2021).
24. Ajinjeru C., Kishore V., Liu P., Lindahl J., Hassen A.A., Kunc V., Post B., Love L. and Duty C., “Determination of melt processing conditions for high performance amorphous thermoplastics for large format additive manufacturing,” Addit. Manuf., 21, 125–132(2018).
25. Acarer-Arat S., Tüfekci M., Pir I. and Tüfekci N., “Nanocellulose in polyvinylidene fluoride (PVDF) membranes: assessing reinforcement impact and modelling techniques,” J. Environ. Chem. Eng., 12, No. 6, 114749(2024).
26. Yang F., Zhang X., Han J. and Du S.Y., “Characterization of hot-pressed short carbon fiber reinforced ZrB2-SiC ultra-high temperature ceramic composites,” J. Alloy. Compd., 472, No. 1–2, 395–399(2009).
27. Yan C., Wei J., Zhu Y.D., Xu H.B., Liu D., Chen G., Liu X.Q., Dai J.Y. and Lv D.X., “Preparation and properties of carbon fiber reinforced bio-based degradable acetal-linkage-containing epoxy resin

composites by RTM process," Polym. Composite., 44, No. 7, 4081–4094(2023).
28. Wang Y., Niu Z.P., Han H.R., Wang J. and Lan D., "Observation of structural, mechanical, thermal and microwave dielectric properties of carbon black reinforced PA6/HDPE nanocomposites," J. Mater. Sci.-Mater. Electron., 34, No. 28, 1948(2023).
29. Ahmad M., Ishak M., Maidin N. and Saharudin M., "Water absorption analysis of oil palm fibre reinforced acrylonitrile butadiene styrene composites by Fick's Law," J. Adv. Res. Exp. Fluid Mech. Heat Transf., 20, No. 1, 150–158(2025).
30. Çavdar S., Sepetcioglu H. and Karagöz İ., "Mechanical, thermal, and morphological properties of nanocellulose reinforced ABS nanocomposites," Cellulose, 31, No. 16, 9715–9729(2024).
31. Karagöz İ., Şimşiroğlu B.Ş., Özer E.N., Sepetcioglu H. and Hızal J., "Investigation of the mechanical, thermal, and morphological properties of ABS composite reinforced with bentonite and DEHPA-modified bentonite," J. Polym. Sci., 63, No. 6, 1505–1517(2025).
32. Lapčík L., Vašina M., Murtaja Y., Sepetcioglu H., Lapčíková B., Ovsík M., Staněk M., Karagöz İ. and Vadanagekar A.S., "ABS nanocomposites for advanced technical and biomedical applications," Polymers, 17, No. 7, 909(2025).
33. Sepetcioglu H., Gunoz A. and Kara M., "Effect of hydrothermal ageing on the mechanical behaviour of graphene nanoplatelets reinforced basalt fibre epoxy composite pipes," Polym. Polym. Compos., 29, No. 9, S166-S177(2021).
34. Sepet H., Aydemir B. and Tarakcioglu N., "Evaluation of mechanical and thermal properties and creep behavior of micro- and nano-$CaCO_3$ particle-filled HDPE nano- and microcomposites produced in large scale," Polym. Bull., 77, No. 7, 3677–3695(2020).
35. Qiao Y.J., Bian X.T., Ke H.J., Zhao Z.Q., Zhang X.H., Zhang X., Zhao Y.K., Bai C.Y., Zhang L.L., Zheng T. and Wang X.D., "Phenolic-based porous composite with embedded short carbon fiber/hollow spheres for mechanical properties and thermostability," Compos. Commun., 55, 102305(2025).
36. Sanjeevi S., Shanmugam V., Kumar S., Ganesan V., Sas G., Johnson D.J., Shanmugam M., Ayyanar A., Naresh K., Neisiany R.E. and Das O., "Effects of water absorption on the mechanical properties of hybrid natural fibre/phenol formaldehyde composites," Sci. Rep., 11, No. 1, 13385(2021).
37. Gupta M.K., "Investigations on jute fibre-reinforced polyester composites: effect of alkali treatment and poly (Lactic Acid) coating," J. Ind. Text., 49, 923–942(2020).
38. Jarukumjorn K. and Suppakarn N., "Effect of glass fiber hybridization on properties of sisal fiber-polypropylene composites," Compos. Part B-Eng., 40, 623–627(2009).
39. Azwa Z.N., Yousif B.F., Manalo A.C. and Karunasena W., "A review on the degradability of polymeric composites based on natural fibres," Mater. Des., 47, 424–442(2013).
40. Dhakal H., Zhang Z. and Richardson M., "Effect of water absorption on the mechanical properties of hemp fibre reinforced unsaturated polyester composites," Compos. Sci. Technol., 67, 1674–1683(2007).
41. Sen I., Aral A., Seki Y., Sarikanat M. and Sever K., "Variations of mechanical properties of jute/polyester composite aged in various media," J. Compos. Mater., 46, 2219–2225(2012).

42. Le Duigou A., Davies P. and Baley C., “Seawater ageing of flax/poly (Lactic Acid) bio-composites,” Polym. Degrad. Stabil., 94, 1151–1162(2009).
43. Gupta M.K. and Srivastava R.K., “Mechanical, thermal and water absorption properties of hybrid sisal/jute fibre reinforced polymer composite,” Indian J. Eng. Mater. Sci., 23, 231–238(2016).
44. Saxena M. and Gupta M.K., “Mechanical, thermal, and water absorption properties of hybrid wood composites,” P. I. Mech. Eng. L-J. Mat., 233, 1914–1922(2018).
45. Wang W., Sain M. and Cooper P.A., “Study of moisture absorption in natural fiber plastic composites,” Compos. Sci. Technol., 66, 379–386(2006).
46. Joseph P.V., Rabello M.S., Mattoso L., Joseph K. and Thomas S., “Environmental effects on the degradation behaviour of sisal fibre reinforced polypropylene composites,” Compos. Sci. Technol., 62, 1357–1372(2002).
47. Manaia J. and Manaia A., “Interface modification, water absorption behaviour and mechanical properties of injection moulded short hemp fiber-reinforced thermoplastic composites,” Polymers, 13, 1638(2021).
48. Wang Q., Chen T., Wang X., Zheng Y., Zheng J., Song G. and Liu S., “Recent progress on moisture absorption aging of plant fiber reinforced polymer composites,” Polymers, 15, No. 20, 4121(2023).
49. Bodur M.S., Englund K. and Bakkal M., “Water absorption behavior and kinetics of glass fiber/waste cotton fabric hybrid composites,” J. Appl. Polym. Sci., 134, No. 47, 45506(2017).

Figures

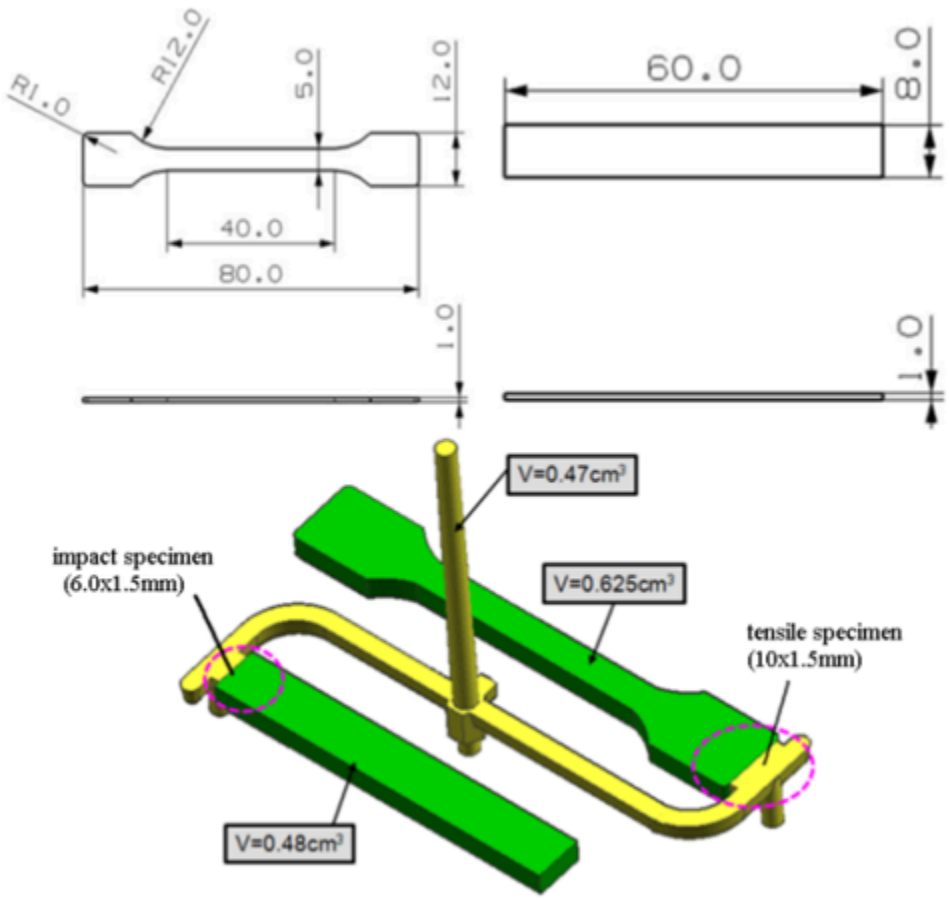

Figure 1

Dimensions of specimens.

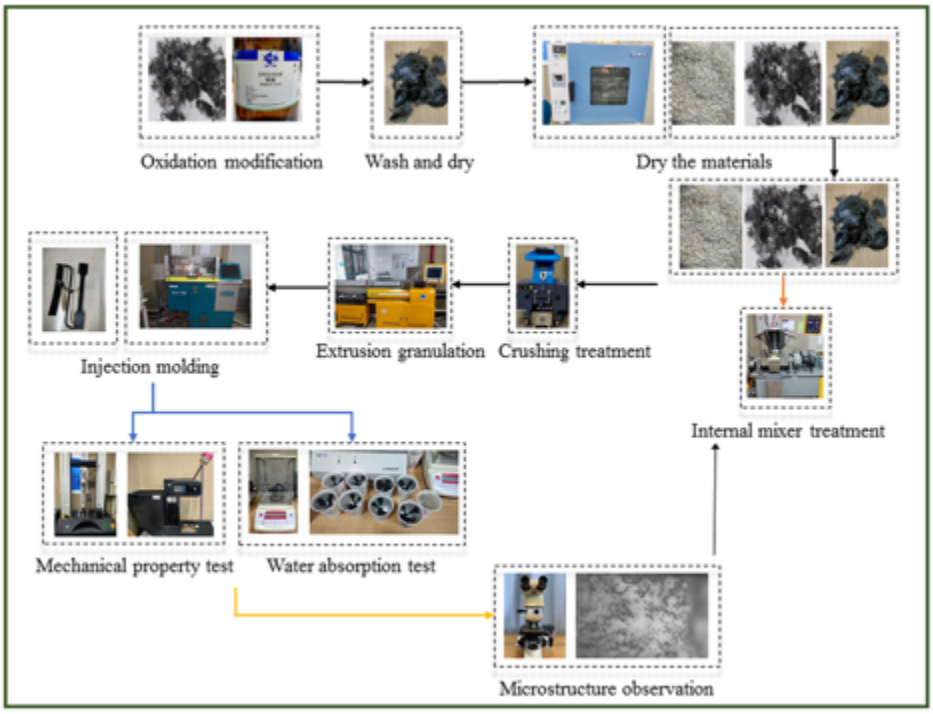

Figure 2

Complete process flow for the preparation and testing of fiber-reinforced composites.

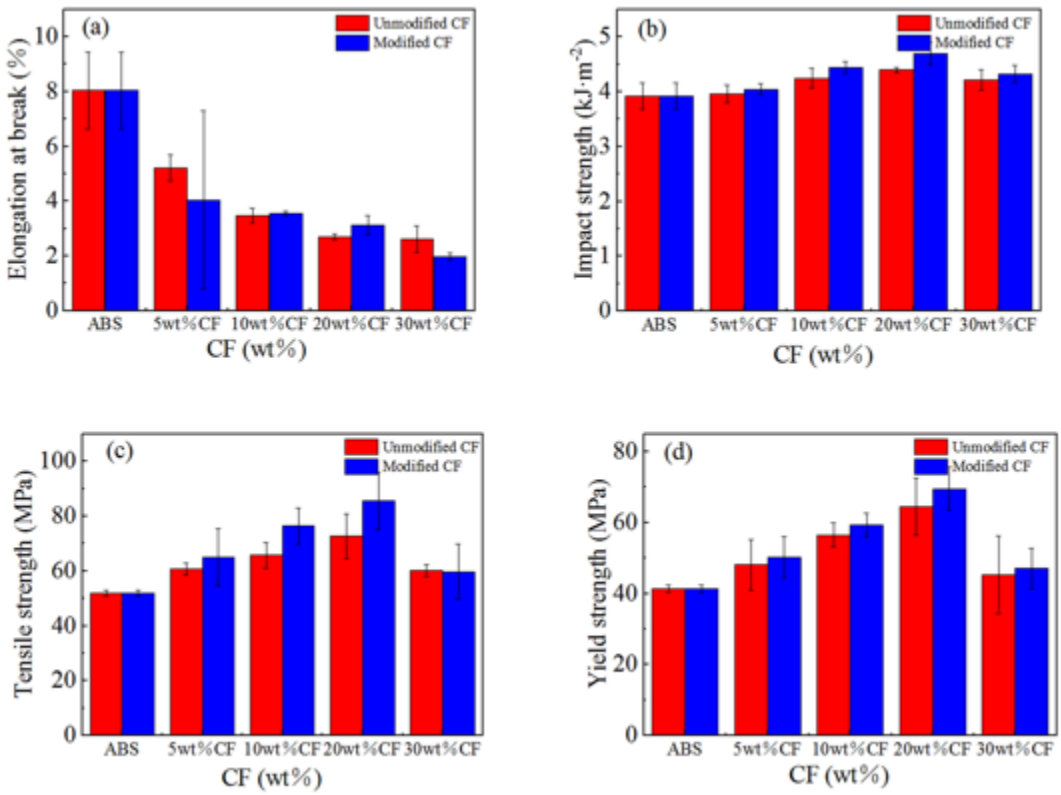

Figure 3

Comparison of mechanical properties of modified and unmodified composites: (a) Elongation at break, (b) Impact strength, (c) Tensile strength, (d) Yield strength.

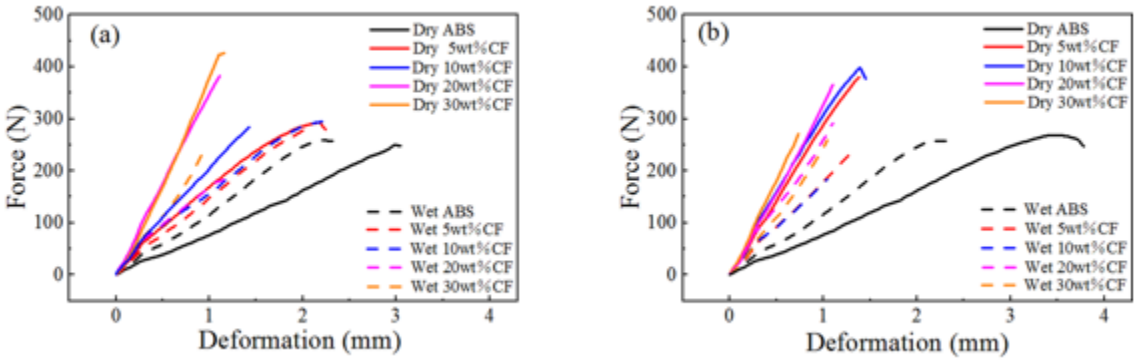

Figure 4

Maximum force–deformation curves of the composites before and after water absorption: (a) Unmodified CF, (b) Modified CF.

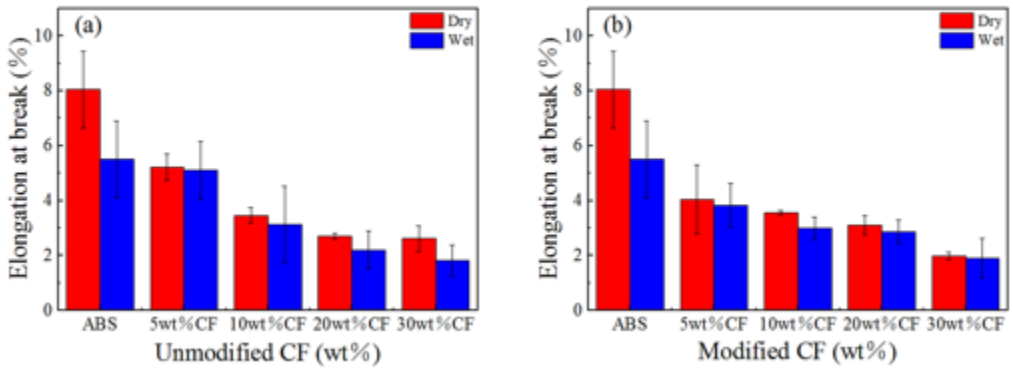

Figure 5

Comparison of elongation at break of composites before and after water absorption: (a) Unmodified CF, (b) Modified CF.

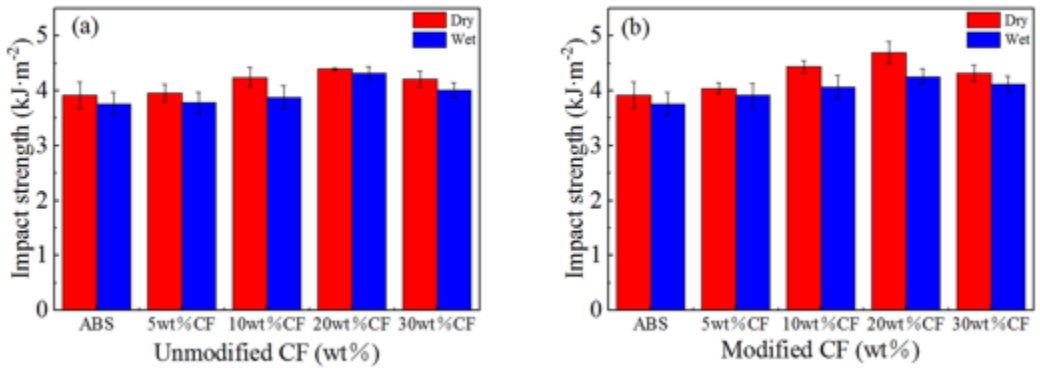

Figure 6

Comparison of impact strength of modified and unmodified composites before and after water absorption: (a) Unmodified CF, (b) Modified CF.

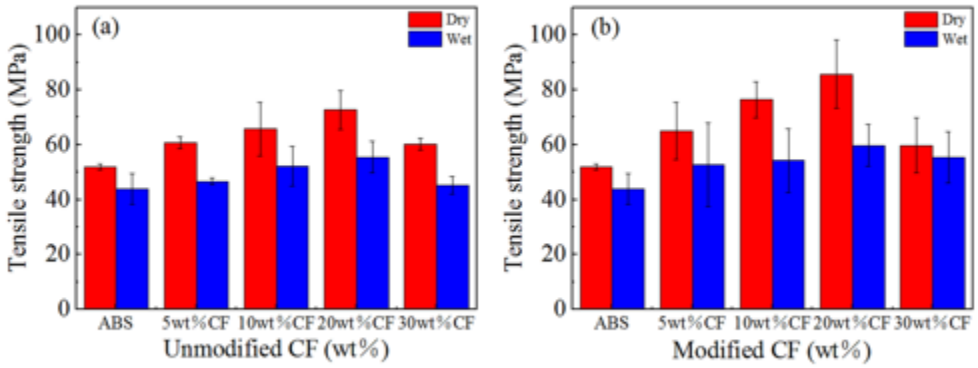

Figure 7

Comparison of tensile strength of modified and unmodified composites before and after water absorption: (a) Unmodified CF, (b) Modified CF.

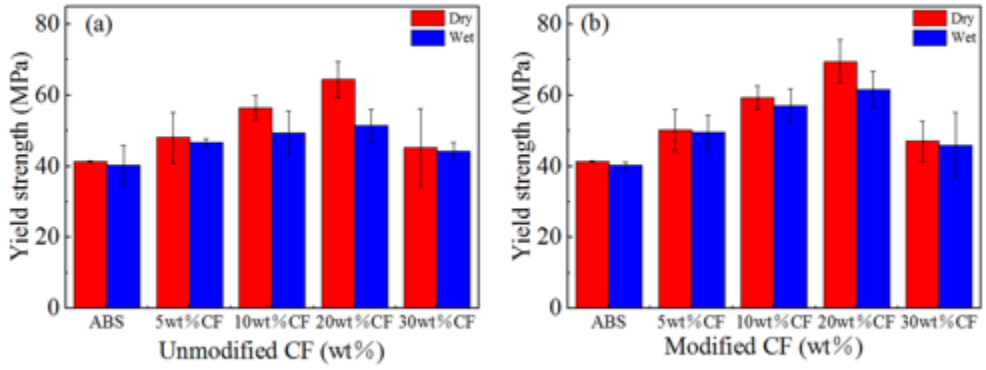

Figure 8

Comparison of yield strength of modified and unmodified composites before and after water absorption: (a) Unmodified CF, (b) Modified CF.

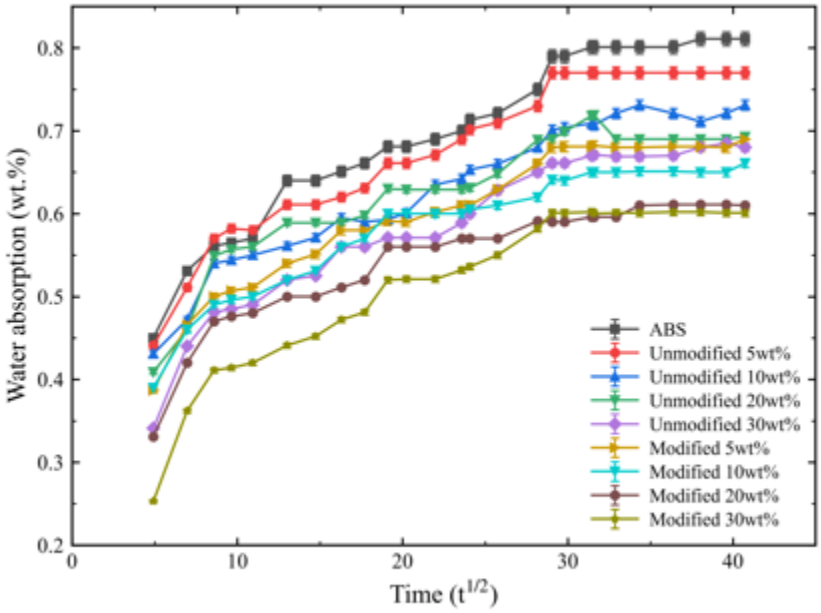

Figure 9

Water-absorption curves of the composites. (Error bars represent the standard deviation (n = 5)).

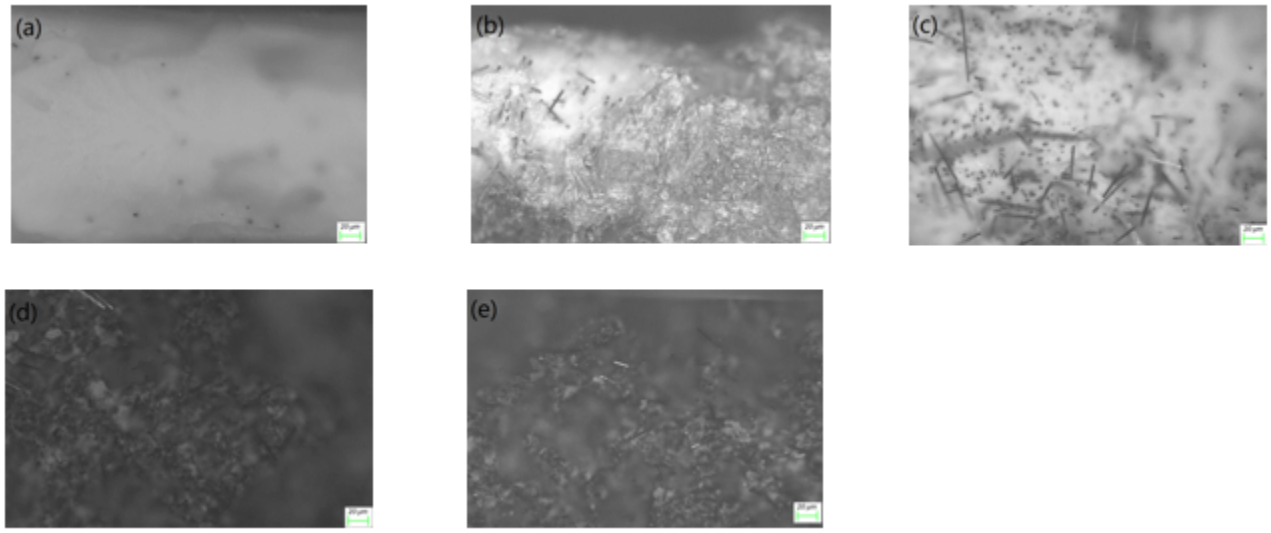

Figure 10

Cross-section micrographs of unmodified composites: (a) ABS, (b) Unmodified 5 wt% CF, (c) Unmodified 10 wt% CF, (d) Unmodified 20 wt% CF, (e) Unmodified 30 wt% CF.

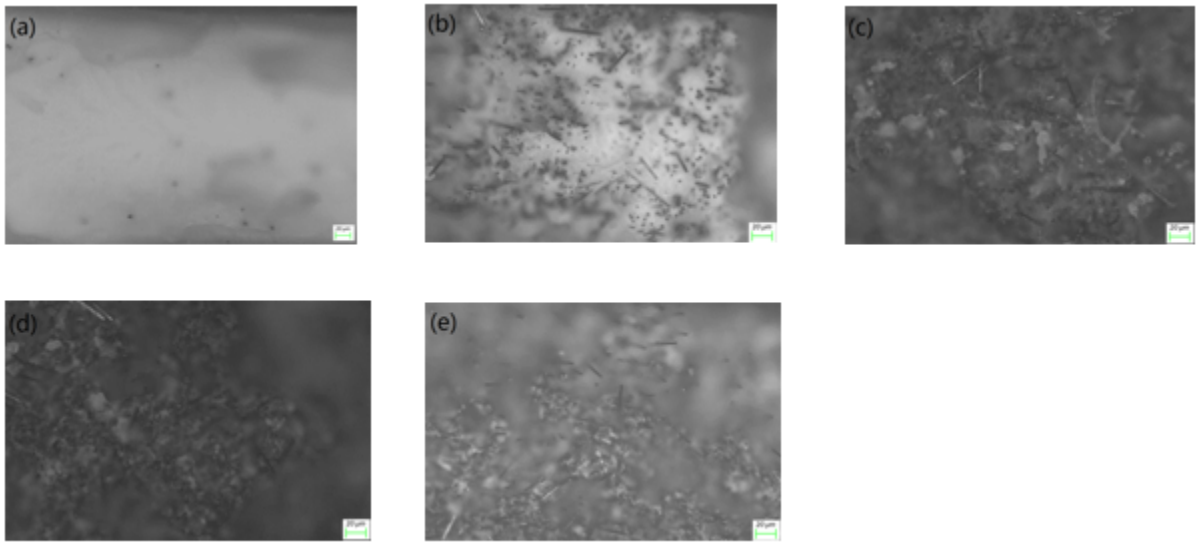

Figure 11

Cross-section micrographs of modified composites: (a) ABS, (b) Modified 5 wt% CF, (c) Modified 10 wt% CF, (d) Modified 20 wt% CF, (e) Modified 30 wt% CF.

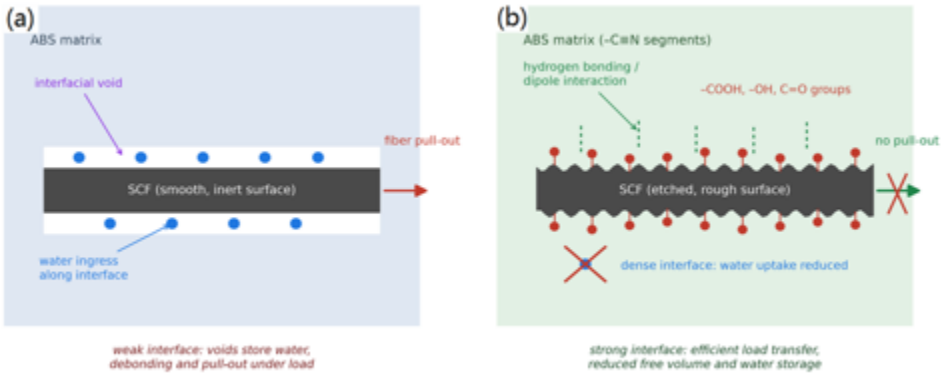

Figure 12

Schematic illustration of the fiber–matrix interface and of the water-transport paths in (a) unmodified and (b) nitric acid-modified SCF/ABS composites.

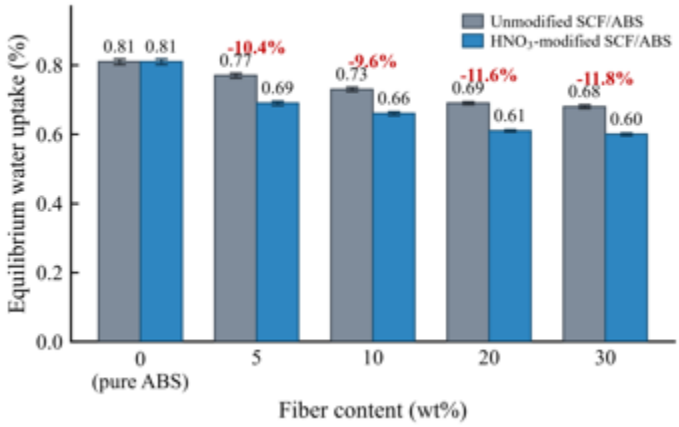

Figure 13

Equilibrium water uptake of unmodified and modified SCF/ABS composites as a function of fiber content (data from Table 3); the percentages give the reduction produced by the nitric acid modification. Error bars represent the standard deviation (n = 5).